NATIONAL ADVISORY COMMITTEE FOR AERONAUTICS

TECHNICAL NOTE

No. 1473

HIGH-SPEED WIND-TUNNEL INVESTIGATION OF HIGH LIFT AND AILERON-CONTROL CHARACTERISTICS OF AN NACA 65-210 SEMISPAN WING

By Jack Fischel and Leslie E. Schneiter

Langley Memorial Aeronautical Laboratory
Langley Field, Va.

Washington
November 1947

NATIONAL ADVISORY COMMITTEE FOR AERONAUTICS

TECHNICAL NOTE NO. 1473

HIGH-SPEED WIND-TUNNEL INVESTIGATION OF HIGH LIFT AND AILERON-CONTROL CHARACTERISTICS OF AN NACA 65-210 SEMISPAN WING

By Jack Fischel and Leslie E. Schneiter

SUMMARY

A high-speed wind-tunnel investigation was made of the aerodynamic characteristics at various Mach numbers of an NACA 65-210 semispan wing variously equipped with a 25-percent-chord full-span slotted flap and a 38-percent-semispan 20-percent-chord straight-sided aileron.

With the full-span flap retracted at a Mach number of 0.13, a maximum lift coefficient of 0.93 was obtained; and with the flap deflected 45°, a maximum lift coefficient of 1.87 was obtained.

The variation of lift with angle of attack C_{L_α} increased from 0.72 at a Mach number of 0.13 to 0.96 at a Mach number of 0.71. This increase in C_{L_α} with Mach number was consistently greater than the increase in C_{L_α} computed by existing theory for finite-span wings.

The effectiveness of the aileron, as shown by the variation of rolling-moment coefficient with aileron deflection $C_{l_{\delta_a}}$, decreased slightly with increase in Mach number and Reynolds number.

Aileron yawing moment became more adverse with increasing angle of attack (or lift) but was essentially unaffected by increasing Mach number.

The variation of the aileron hinge-moment coefficient with angle of attack C_{h_α} increased positively from -0.0008 at a Mach number of 0.27 to 0.0010 at a Mach number of 0.71; whereas the variation of the hinge-moment coefficient with aileron deflection $C_{h_{\delta_a}}$ increased negatively from -0.0052 at a Mach number of 0.27 to -0.0072 at a Mach number of 0.71.

INTRODUCTION

The necessity of providing sufficiently high lift for landing and take-off, as well as adequate lateral control throughout the flight speed range for the fast and heavily loaded airplanes currently in use or in the design stage, has presented a problem to airplane designers. This problem has been accentuated somewhat by the required use of wings having high critical speeds and by the paucity of existing lift and lateral-control data on finite-span wings. In order to assist in solving this problem, an investigation was conducted in the Langley high-speed 7- by 10-foot tunnel on a thin low-drag semispan wing (NACA 65-210) equipped with either a full-span slotted flap or a partial-span aileron. Wing lift, drag, and pitching-moment characteristics were obtained through a speed range to a Mach number of 0.71 with the full-span flap retracted and through a speed range to a Mach number of 0.27 with the flap deflected. Tests of a 0.38-semispan 0.20-chord straight-sided aileron were made at various speeds up to a Mach number of 0.71.

SYMBOLS

The moments on the wing are presented about the wind axes. The X-axis is in the plane of symmetry of the model and is parallel to the tunnel air flow. The Z-axis is in the plane of symmetry and is perpendicular to the X-axis. The Y-axis is mutually perpendicular to the X- and Z-axes. All three axes intersect at the intersection of the chord plane and the 35-percent-chord station at the root of the model.

The symbols used in the presentation of results are as follows:

C_L lift coefficient $\left(\frac{\text{Twice lift of semispan model}}{qS}\right)$

C_D drag coefficient (D/qS)

C_m pitching-moment coefficient $\left(\frac{\text{Twice pitching moment of semispan model}}{qSc}\right)$

C_l rolling-moment coefficient (L/qSb)

C_n yawing-moment coefficient (N/qSb)

C_h aileron hinge-moment coefficient $\left(H_a/qb_a\bar{c}_a^2\right)$

c local wing chord

c' wing mean aerodynamic chord, 2.86 feet $\left(\frac{2}{S}\int_0^{b/2} c^2\,dy\right)$

c_a aileron chord measured along wing chord line from hinge axis of aileron to trailing edge of wing

$\overline{c_a}$ root-mean-square chord of aileron, 0.48 foot

b twice span of semispan model, 16 feet

b_a aileron span, 3.04 feet

y lateral distance from plane of symmetry, feet

S twice area of semispan model, 44.42 square feet

D twice drag of semispan model, pounds

L rolling moment due to aileron deflection about X-axis, foot-pounds

N yawing moment due to aileron deflection about Z-axis, foot-pounds

H_a aileron hinge moment, foot pounds

q free-stream dynamic pressure, pounds per squre foot $\left(\frac{1}{2}\rho V^2\right)$

V free-stream velocity, feet per second

ρ mass density of air, slugs per cubic foot

α angle of attack with respect to chord plane at root of model, degrees

δ_a aileron deflection relative to wing chord plane (positive when trailing edge is down), degrees

δ_f flap deflection relative to wing chord plane (positive when trailing edge is down), degrees

M Mach number (V/a)

R Reynolds number

a speed of sound, feet per second

$$C_{h_\alpha} = \left(\frac{\partial C_h}{\partial \alpha}\right)_{\delta_a}$$

$$C_{h_{\delta_a}} = \left(\frac{\partial C_h}{\partial \delta_a}\right)_{\alpha}$$

$$C_{L_\alpha} = \left(\frac{\partial C_L}{\partial \alpha}\right)_{\delta_a}$$

$$C_{l_{\delta_a}} = \left(\frac{\partial C_l}{\partial \delta_a}\right)_{\alpha}$$

The subscripts δ_a and α indicate the factor held constant. All slopes were measured in the vicinity of 0° angle of attack and 0° aileron deflection.

CORRECTIONS

With the exception of the aileron hinge-moment data, all data presented are based on the dimensions of the complete wing.

The test data have been corrected for jet-boundary effects according to the methods outlined in reference 1. Compressibility effects on these jet-boundary corrections have been considered in correcting the test data; blockage corrections were also applied.

Aileron deflections have been corrected for deflection under load, and the aileron data have been corrected for the small amount of wing twist (less than 0.2°) produced by aileron deflection.

MODEL AND APPARATUS

The semispan-wing model was mounted in inverted position in the Langley high-speed 7- by 10-foot tunnel with its root section adjacent to one of the vertical walls of the tunnel, the vertical wall thereby serving as a reflection plane (figs. 1 and 2). The wing was cantilever supported from the balance frame near the wing root section,

and a gap of approximately 1/16 inch between the tunnel wall and the root end of the model permitted all forces and moments acting on the model to be measured.

The semispan wing model was built to the plan-form dimensions shown in figure 3 and had an NACA 65-210 airfoil section (table I) from root to tip with neither twist nor dihedral. The model had an aspect ratio of 5.76 and a ratio of tip chord to root chord of 0.57. The wing plan form exclusive of the aileron dimensions was geometrically similar to the quarter span of a complete wing model of aspect ratio 9 used in several investigations for which the data are unpublished. The wing was fabricated with a solid steel spar and laminated-mahogany surfaces. No transition strips were used on the wing, and an attempt was made to keep the model surface smooth during the entire investigation.

The full-span slotted-flap configuration was built to the dimensions given in figure 3 and is shown mounted on the wing in the tunnel test section in figure 1. The design dimensions for the 0.25c flap are presented in table I and agree with the dimensions for slotted flap 1 given in reference 2. The optimum flap position with respect to the upper-surface airfoil lip and the optimum flap deflection ($\delta_f = 45^\circ$) given in reference 2 were used for the normal flap-deflected position in the present investigation. The flap had a solid steel spar with laminated-mahogany surfaces.

The partial-span aileron configuration was built to the dimensions given in figure 4, and the configuration is shown in the tunnel in figure 2. The aileron of $0.38\frac{b}{2}$ and 0.20c was constructed of duralumin and had straight sides and a trailing-edge angle of 11°. The aileron had a plain radius-nose overhang made of mahogany and was tested with a plastic-impregnated fabric seal across the gap ahead of the aileron nose, except at the location of the strain-gage arm where a gap of about $0.01\frac{b}{2}$ existed. In addition, the aileron was equipped with strain-gage beams of various sizes to provide a maximum of sensitivity to the hinge-moment readings at the various deflections and speeds at which the investigation was made. Aileron deflection was set for each test by means of a beam-type clamp strain-gage arm.

The Langley high-speed 7- by 10-foot tunnel is a closed-throat single-return tunnel. The turbulence of the tunnel air stream has not been determined but is thought to be low because of the large tunnel contraction ratio (14 to 1). This belief is substantiated by turbulence measurements made in the Langley 300 MPH 7- by 10-foot tunnel.

TESTS

Wing angle-of-attack tests with the flap retracted were made through a Mach number range from 0.13 to 0.71, with a corresponding Reynolds number range of approximately 2.6×10^6 to 10.3×10^6 based on a mean aerodynamic chord of 2.86 feet. In addition, a constant angle-of-attack (approximately at zero lift) speed test was made through a Mach number range from 0.44 to 0.82. Wing angle-of-attack tests with the flap deflected were made through a Mach number range from 0.13 to 0.27. The variation of Reynolds number with Mach number for these tests is shown in figure 5.

Tests were made with various aileron deflections through an angle-of-attack range at Mach numbers from 0.27 to 0.71. The range of aileron angles tested was between approximately -15° and 15°, except at the lower values of Mach number where a deflection range of approximately -15° to 20° was used. The angle-of-attack range covered in all the tests became more limited as Mach number increased because of the load limitations of the model.

DISCUSSION

Wing Aerodynamic Characteristics

The lift, drag, and pitching-moment characteristics of the wing model at various Mach numbers in the flap-retracted and flap-deflected configurations are shown in figures 6 and 7, respectively. As Mach number increased in the flap-retracted configuration, a gradual increase in the lift-curve slope, a small increase in drag coefficient at low lift coefficients, and very little change in pitching-moment characteristics were obtained. Maximum lift coefficients of 0.93 and 1.87 were obtained at a Mach number of 0.13 with the full-span flap retracted and deflected, respectively.

In order to ascertain whether the normal flap position used was optimum for three-dimensional flow, several additional tests were made in which the flap deflection was held constant at 45° and the location of the flap nose with respect to the wing upper-surface lip was varied. The results presented in figure 8 show that, in general, moving the flap down and back from the normal flap-deflected position (nose of flap 0.0100c below and ahead of wing upper-surface lip) resulted in a decrease in lift and an increase in drag at all angles of attack, except for the configuration in which the outboard end of the flap was held in the normal position and the flap nose at the inboard end was moved rearward and down from the normal positon,

a change which enlarged the gap between the flap and the wing lip. For this wing-flap configuration, a larger maximum lift was noted than for the normal wing-flap configuration. (See fig. 8.) Sealing the flap slot in one of these configurations was quite deleterious in that a large decrease in lift and an increase in drag resulted.

Variation of the lift-curve slope C_{L_α} with Mach number is shown in figure 9, in which a steady increase of C_{L_α} with Mach number is apparent; that is, C_{L_α} increased from 0.72 at $M = 0.13$ to 0.96 at $M = 0.71$. No force break induced by a wing shock was apparent within the lift range covered. (See figs. 6 and 9.) The data of figure 9 also compare the compressibility effects on C_{L_α} obtained from experimental data with the results computed by the Prandtl-Glauert factor, which is based on two-dimensional flow, and those computed by an equation derived by Young of Great Britain for finite-span wings and revised by Jones' edge-velocity correction (reference 3). The increase in lift-curve slope with increasing Mach number obtained in the investigation was consistently greater than that computed by the revised Young equation.

Variation of the lift, drag, and pitching-moment coefficients with Mach number at a constant angle of attack approximately corresponding to zero lift is shown in figure 10. From these data and the data of figures 6 and 9, a positive shift of the angle of zero lift and a rearward shift of the center of pressure with increasing Mach number is indicated. A gradual increase in the drag coefficient at Mach numbers above 0.75 apparently indicates the approaching existence or the existence of shock on the wing.

Aileron-Control Characteristics

The results of the investigation of the aileron-control characteristics at various Mach numbers are shown plotted against wing angle of attack in figure 11 and cross-plotted against aileron deflection at three low angles of attack in figure 12.

The rolling-moment data generally show a decrease in effectiveness with angle-of-attack increase for positive aileron deflections at the lower Mach numbers ($M = 0.27$ and 0.38) and an inconsistent effect in the negative aileron-deflection range. For Mach numbers above 0.38, the aileron effectiveness generally increases slightly with angle-of-attack increase for both positive and negative aileron deflections. (See fig. 11.) The data of figure 11 further show a decrease in aileron effectiveness with increase in Mach number, and this phenomenon is more clearly illustrated in figures 12 and 13. This variation of

aileron effectiveness with Mach number is opposite to that obtained in an aileron investigation for a wing of aspect ratio 9 employing the same airfoil section (unpublished data).

Some of this discrepancy is explained by the fact that the data for the wing of aspect ratio 9 were not corrected for wind-tunnel jet-boundary effects. Moreover, the validity of jet-boundary corrections for reflection-plane models at high Mach numbers has not been well-established; as a consequence, the corrections applied to the present data at high Mach numbers are questionable but are thought to be conservative.

In addition, some of this discrepancy is attributed to the fact that the data obtained in the investigation of the wing of aspect ratio 9 were at Reynolds numbers from 0.9×10^6 to 1.4×10^6, whereas the Reynolds number range of the aileron investigation reported herein was between approximately 5.2×10^6 and 10.3×10^6. Two-dimensional tests of a 0.20c straight-sided aileron on the same airfoil section (reference 4) at Reynolds numbers of 1×10^6 and 9×10^6 (Mach numbers of 0.07 and 0.17, respectively) indicated that a slight decrease in aileron effectiveness resulted when the Reynolds number increased; whereas high-speed aileron tests of the the same airfoil section within a Reynolds number range of 1×10^6 to 2×10^6 indicated that an increase in Mach number and Reynolds number increased the aileron effectiveness. It is believed, therefore, that the discrepancy in the aileron effectiveness exhibited between the data presented herein and the data obtained from the wing of aspect ratio 9 probably result from a Reynolds number effect, which is either negligible or similar to a Mach number effect at low Reynolds numbers and opposite to a Mach number effect at high Reynolds numbers. A part of this discrepancy may also result from the fact that the aerodynamic effects which accompany a reduction in effective aspect ratio resulting from compressibility effects are larger for the wing of aspect ratio 5.76 than for the wing of aspect ratio 9. This belief is substantiated somewhat by similar effects shown by the results of a lateral-control investigation (reference 5) performed on a thicker semispan wing at Reynolds numbers and Mach numbers (over the span of the aileron tested) which are comparable to those existing during the reported investigation. These results are reproduced in figure 13 for comparison with the reported data.

A comparison of the aileron-effectiveness (indicated by the slope $C_{l_{\delta_a}}$) obtained in the present investigation at a Mach number

of 0.38 was made with the aileron effectiveness obtained from the wing of aspect ratio 9 at the same Mach number. Good agreement between the two investigations was obtained after accounting for aspect-ratio differences by use of reference 6 and correcting the data of the wing of aspect ratio 9 for jet-boundary effects by use of reference 1. At higher Mach numbers, Reynolds number effects on aileron effectiveness and compressibility effects on effective aspect ratio (as previously discussed) probably account for the poorer agreement as Mach number increased.

The aileron yawing-moment coefficients varied almost linearly with angle of attack (or lift) and generally became more adverse as the angle of attack increased, particularly in the positive aileron-deflection range. (See figs. 11 and 12.) Mach number had almost no effect on the yawing-moment coefficients.

The aileron hinge-moment coefficients also varied almost linearly with angle of attack, and the value of C_{h_α} increased positively with increase in Mach number from -0.0008 at $M = 0.27$ to 0.0010 at $M = 0.71$. (See figs. 11 and 13.) The variation of hinge-moment coefficient with aileron deflection tended to become more nearly linear as the Mach number increased (fig. 12), and the value of $C_{h_{\delta_a}}$ increased negatively with increase in the Mach number from -0.0052 at $M = 0.27$ to -0.0072 at $M = 0.71$. (See fig. 13.) A comparison of the values of C_{h_α} and $C_{h_{\delta_a}}$ obtained in the present investigation with the values obtained in the investigation of the wing of aspect ratio 9 (data unpublished) indicated that these parameters were less negative and exhibited larger compressibility effects in the present investigation. The differences in the results obtained in the two investigations may be attributed to differences in aspect ratio, Reynolds number, and the fact that the aileron nose gap was not sealed in the investigation of the wing of aspect ratio 9 but was sealed in the present investigation.

No data were obtained for pressures across the aileron seal. It is believed, however, since the aileron tested had its nose gap fairly well sealed that the equations presented in reference 7 may be used to compute various balance configurations required for given stick forces.

CONCLUSIONS

A high-speed wind-tunnel investigation was made of the aerodynamic characteristics at various Mach numbers of an NACA 65-210 semispan wing

variously equipped with a 25-percent-chord full-span slotted flap and a 38-percent-semispan 20-percent-chord straight-sided aileron. The results of the investigation led to the following conclusions:

1. With the full-span flap retracted at a Mach number of 0.13, a maximum lift coefficient of 0.93 was obtained; and with the flap deflected 45°, a maximum lift coefficient of 1.87 was obtained.

2. The variation of lift with angle of attack C_{L_α} increased from 0.72 at a Mach number of 0.13 to 0.96 at a Mach number of 0.71. This increase in C_{L_α} with Mach number was consistently greater than the increase in C_{L_α} computed by existing theory for finite-span wings.

3. The effectiveness of the aileron, as shown by the variation of rolling-moment coefficient with aileron deflection $C_{l_{\delta_a}}$, decreased slightly with increase in Mach number and Reynolds number.

4. Aileron yawing moment became more adverse with increasing angle of attack (or lift) but was essentially unaffected by increasing Mach number.

5. The variation of the aileron hinge-moment coefficient with angle of attack C_{h_α} increased positively from -0.0008 at a Mach number of 0.27 to 0.0010 at a Mach number of 0.71; whereas the variation of the hinge-moment coefficient with aileron deflection $C_{h_{\delta_a}}$ increased negatively from -0.0052 at a Mach number of 0.27 to -0.0072 at a Mach number of 0.71.

Langley Memorial Aeronautical Laboratory
National Advisory Committee for Aeronautics
Langley Field, Va., July 3, 1947

REFERENCES

1. Swanson, Robert S., and Toll, Thomas A.: Jet-Boundary Corrections for Reflection-Plane Models in Rectangular Wind Tunnels. NACA ARR No. 3E22, 1943.

2. Cahill, Jones F.: Two-Dimensional Wind-Tunnel Investigation of Four Types of High-Lift Flaps on an NACA 65-210 Airfoil Section. NACA TN No. 1191, 1947.

3. Jones, Robert T.: Theoretical Correction for the Lift of Elliptic Wings. Jour. Aero. Sci., vol. 9, no. 1, Nov. 1941, pp. 8-10.

4. Underwood, William J., Braslow, Albert L., and Cahill, Jones F.: Two-Dimensional Wind-Tunnel Investigation of 0.20-Airfoil-Chord Plain Ailerons of Different Contour on an NACA 65_1-210 Airfoil Section. NACA ACR No. L5F27, 1945.

5. Laitone, Edmund V., and Summers, James L.: An Additional Investigation of the High-Speed Lateral-Control Characteristics of Spoilers. NACA ACR No. 5D28, 1945.

6. Pearson, Henry A., and Jones, Robert T.: Theoretical Stability and Control Characteristics of Wings with Various Amounts of Taper and Twist. NACA Rep. No. 635, 1938.

7. Langley Research Department: Summary of Lateral-Control Research. (Compiled by Thomas A. Toll.) NACA TN No. 1245, 1947.

TABLE I.- ORDINATES FOR AIRFOIL AND FLAP

[All dimensions in percent of wing chord]

NACA 65-210 airfoil section

Upper surface		Lower surface	
Station	Ordinate	Station	Ordinate
0	0	0	0
.435	.819	.565	-.719
.678	.999	.822	-.859
1.169	1.273	1.331	-1.059
2.408	1.757	2.592	-1.385
4.893	2.491	5.102	-1.859
7.394	3.069	7.606	-2.221
9.894	3.555	10.106	-2.521
14.899	4.338	15.101	-2.992
19.909	4.938	20.091	-3.346
24.921	5.397	25.079	-3.607
29.936	5.732	30.064	-3.788
34.951	5.954	35.049	-3.894
39.968	6.067	40.032	-3.925
44.984	6.058	45.016	-3.868
50.000	5.918	50.000	-3.709
55.014	5.625	54.986	-3.435
60.027	5.217	59.973	-3.075
65.036	4.712	64.964	-2.652
70.043	4.128	69.957	-2.184
75.045	3.479	74.955	-1.689
80.044	2.783	79.956	-1.191
85.038	2.057	84.962	-.711
90.028	1.327	89.972	-.293
95.014	.622	94.986	.010
100.000	0	100.000	0

L.E. radius: 0.687
Slope of radius through L.E.: 0.084

NATIONAL ADVISORY
COMMITTEE FOR AERONAUTICS

TABLE I.- ORDINATES FOR AIRFOIL AND FLAP - Concluded

[All dimensions in percent of wing chord]

Slotted flap

Upper surface		Lower surface	
Station	Ordinate	Station	Ordinate
0	0	0	0
.28	.92	.28	-.41
.56	1.19	.56	-.62
1.12	1.56	1.12	-.88
1.69	1.80	1.69	-1.00
2.25	1.99	2.48	-1.03
3.38	2.22	4.98	-.83
4.50	2.33	7.48	-.63
5.61	2.38	9.98	-.44
7.00	2.40	12.48	-.27
9.00	2.35	14.98	-.12
11.00	2.16	17.48	.01
12.51	1.91	19.99	.10
15.01	1.50	22.49	.12
17.51	1.10	25.00	0
20.00	.71		
22.50	.34		
25.00	0		

L.E. radius: 0.80
Slope of radius through L.E.: 0.35

NATIONAL ADVISORY
COMMITTEE FOR AERONAUTICS

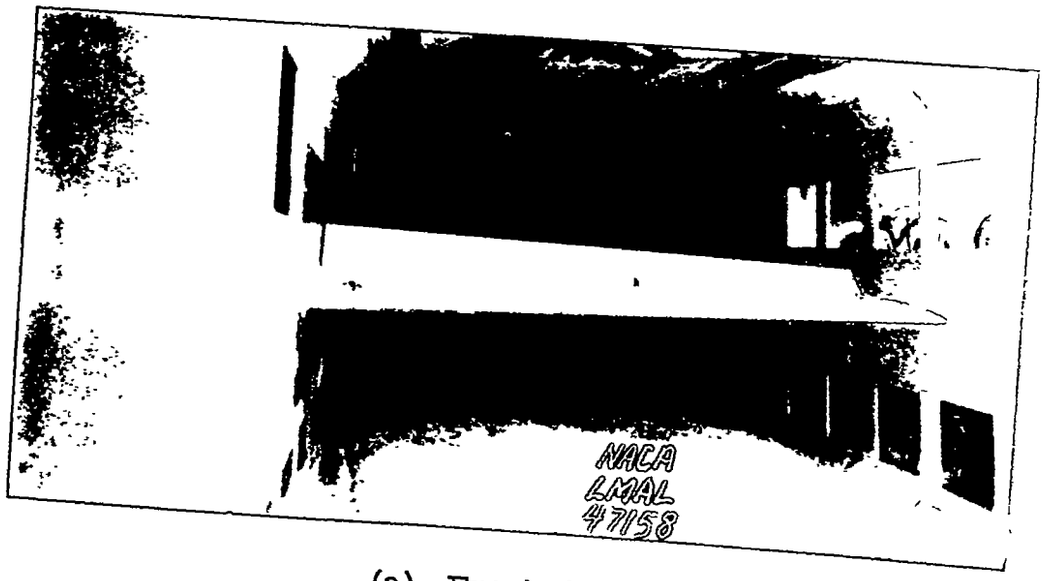

(a) Front view.

Figure 1.- Reflection-plane model in inverted position with full-span flap deflected.

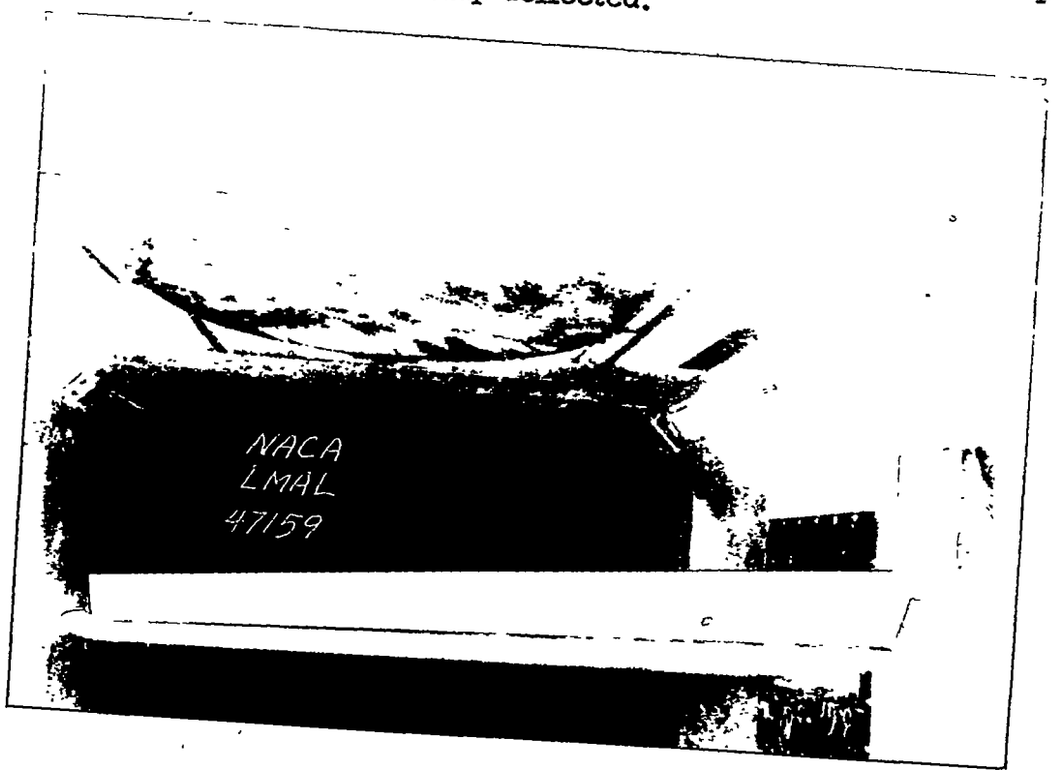

(b) Rear view.

Figure 1.- Concluded.

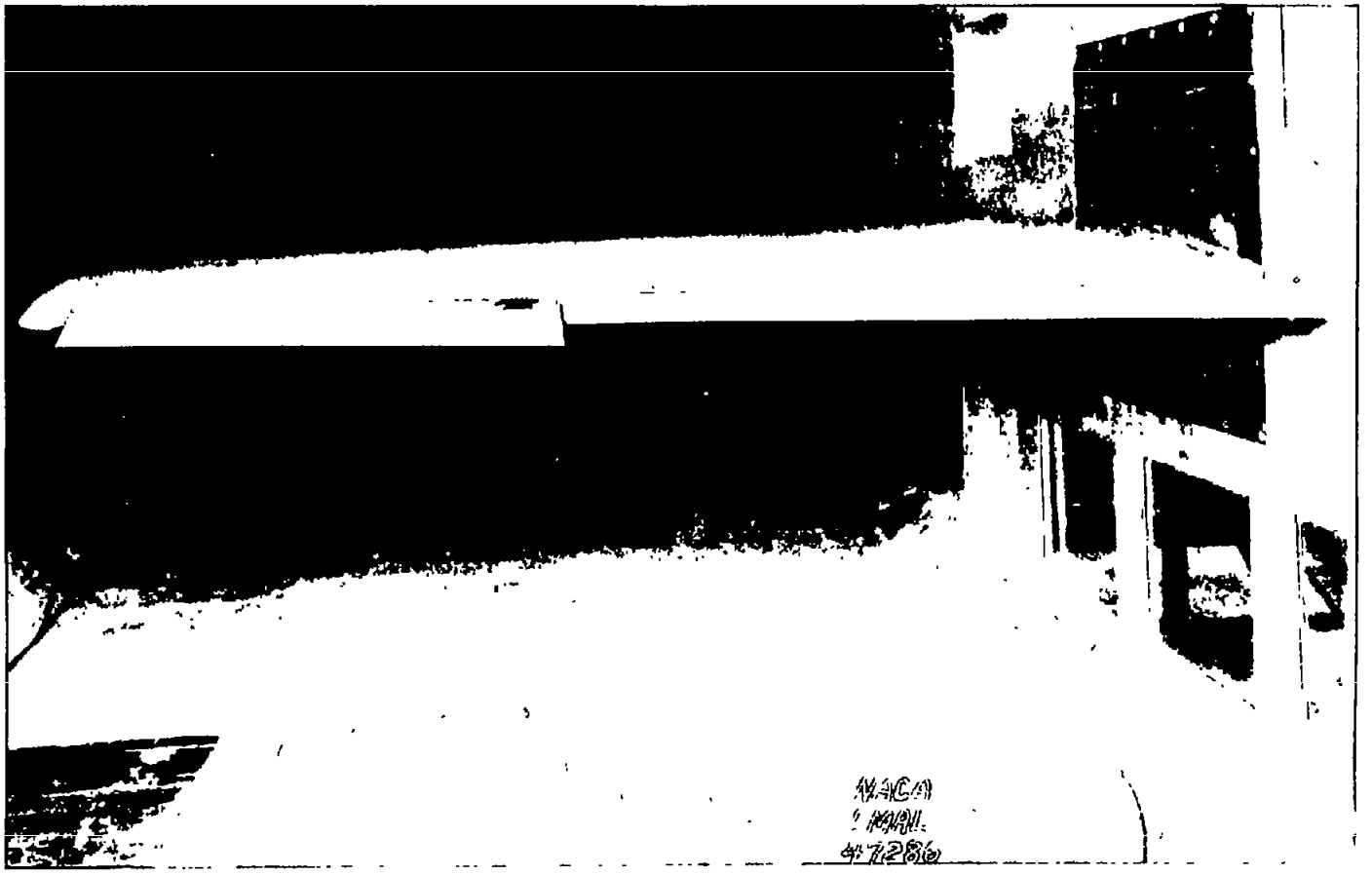

Figure 2.- Rear view of reflection-plane model in inverted position with aileron deflected.

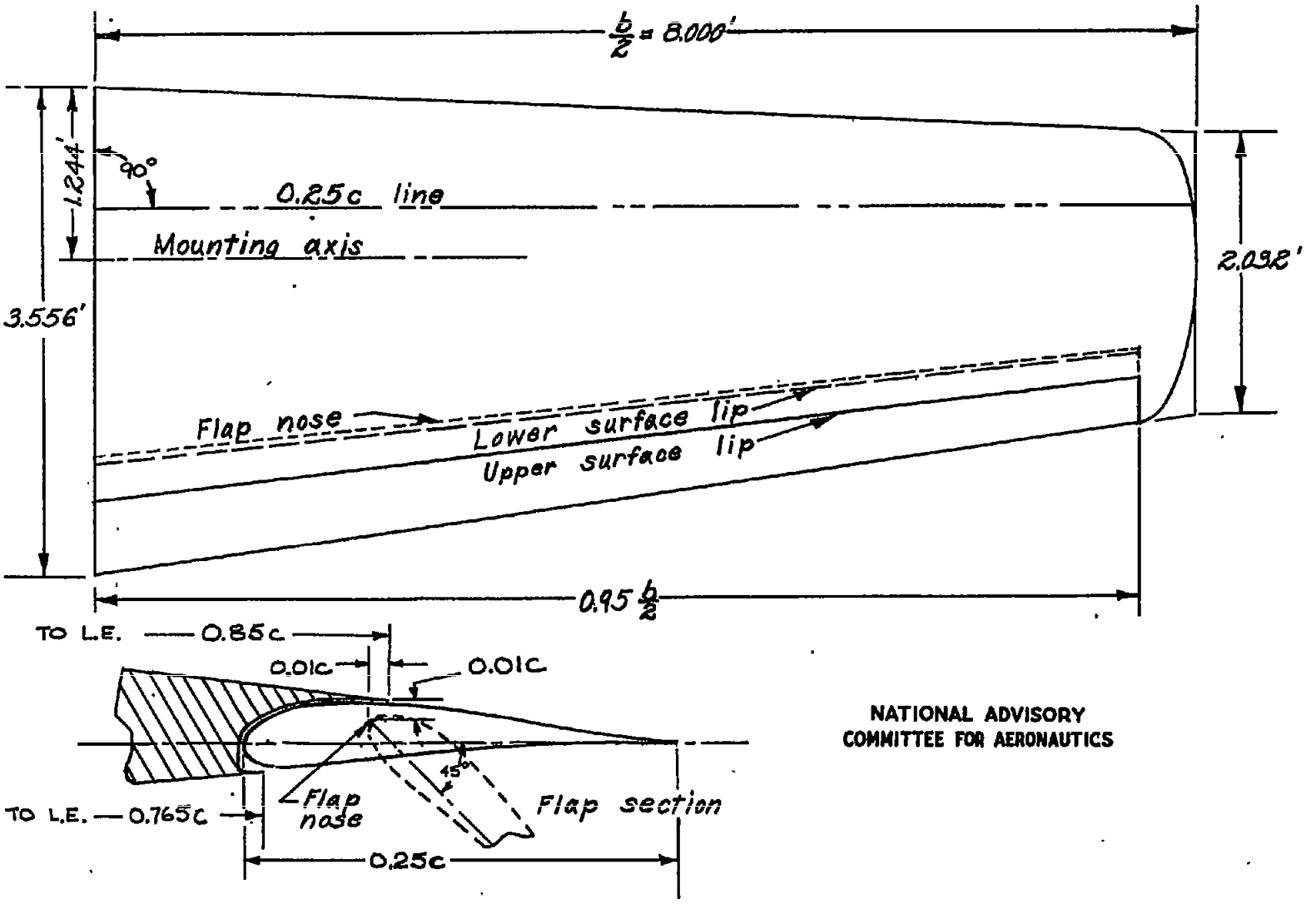

Figure 3.- Schematic drawing of right semispan-wing model equipped with full-span flap.

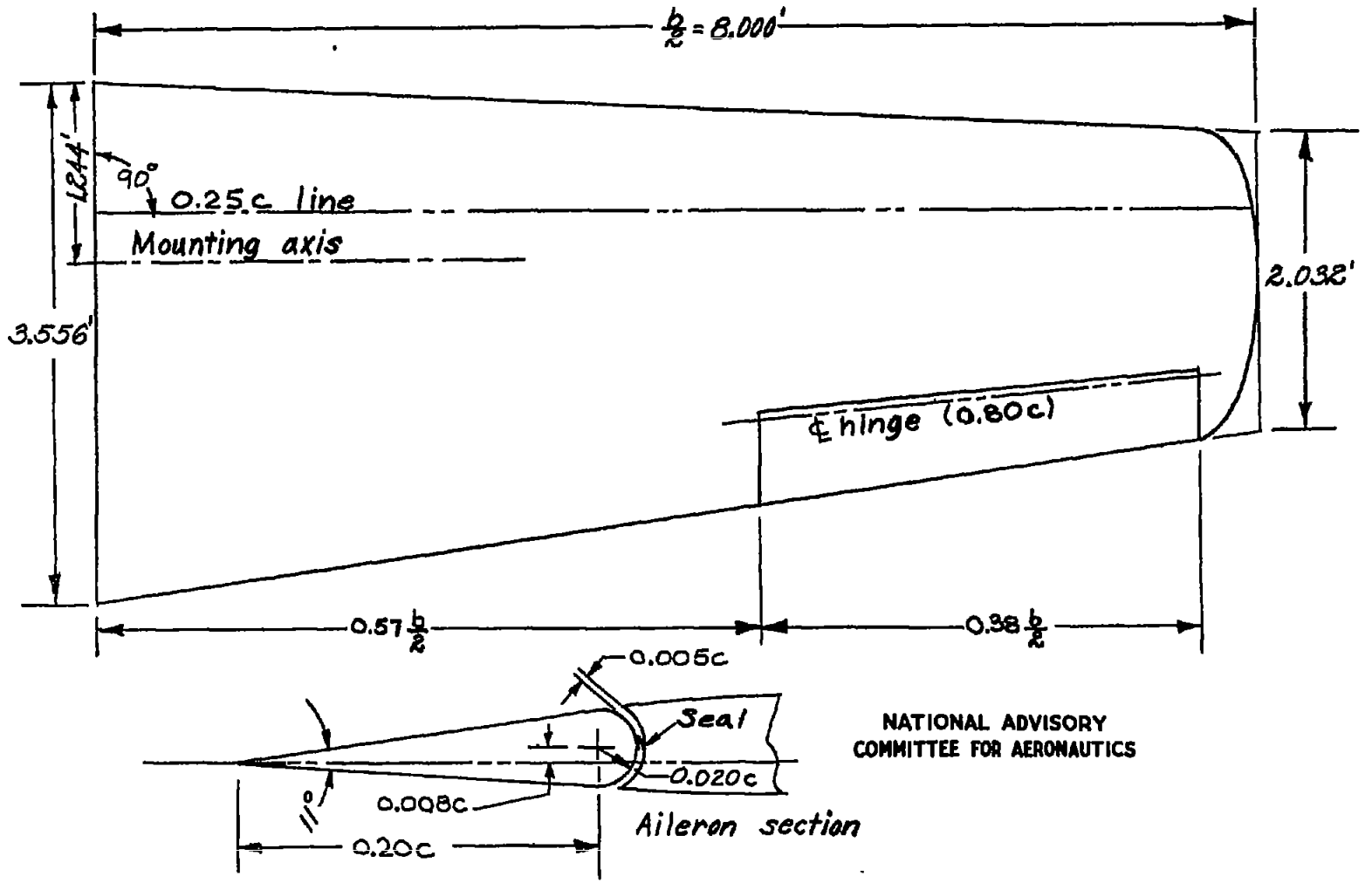

Figure 4.- Schematic drawing of right semispan-wing model equipped with 38-percent semispan aileron having straight-sided airfoil contour.

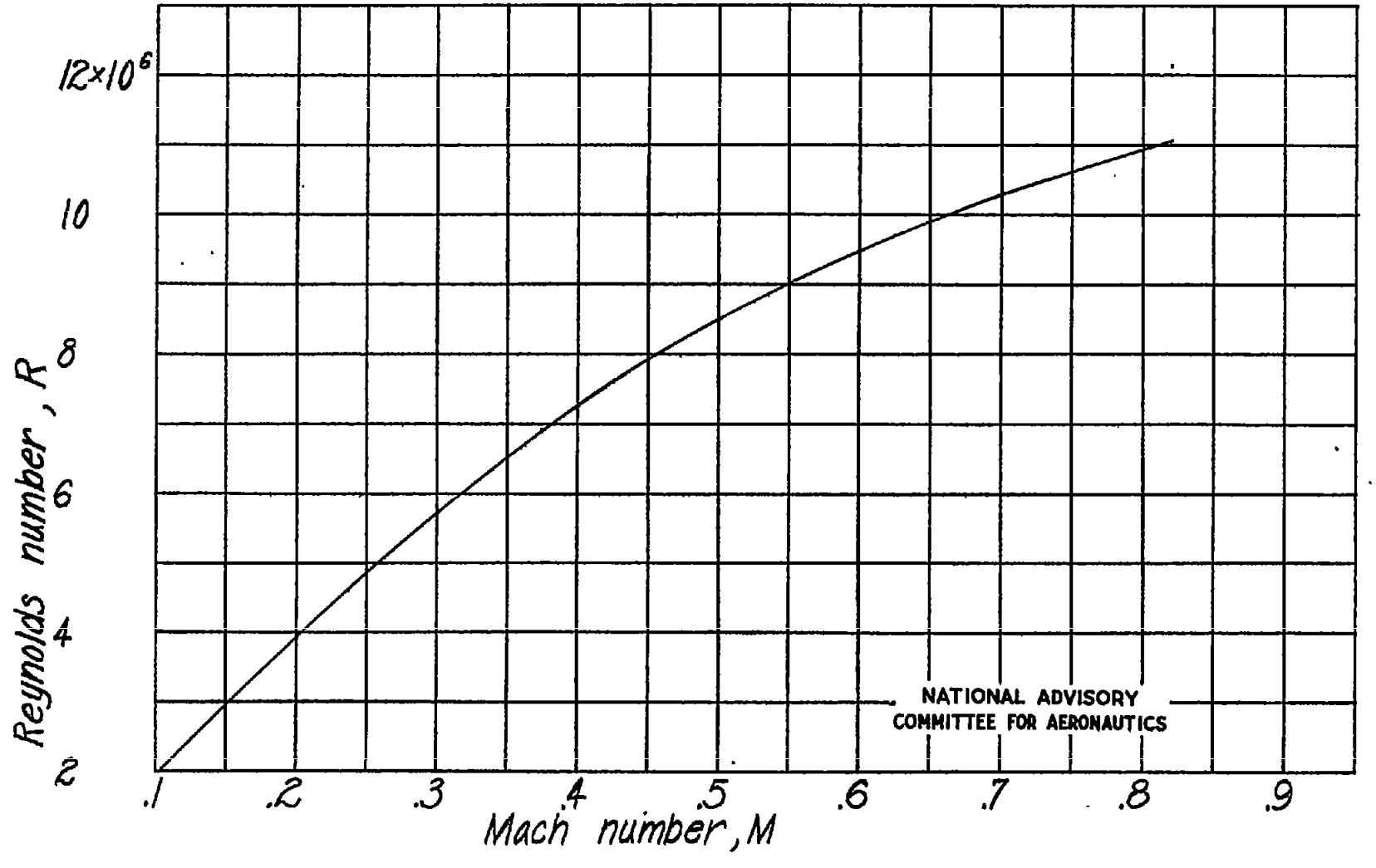

Figure 5.- Variation of Reynolds number with Mach number. Reynolds number is based on wing mean aerodynamic chord of 2.86 feet.

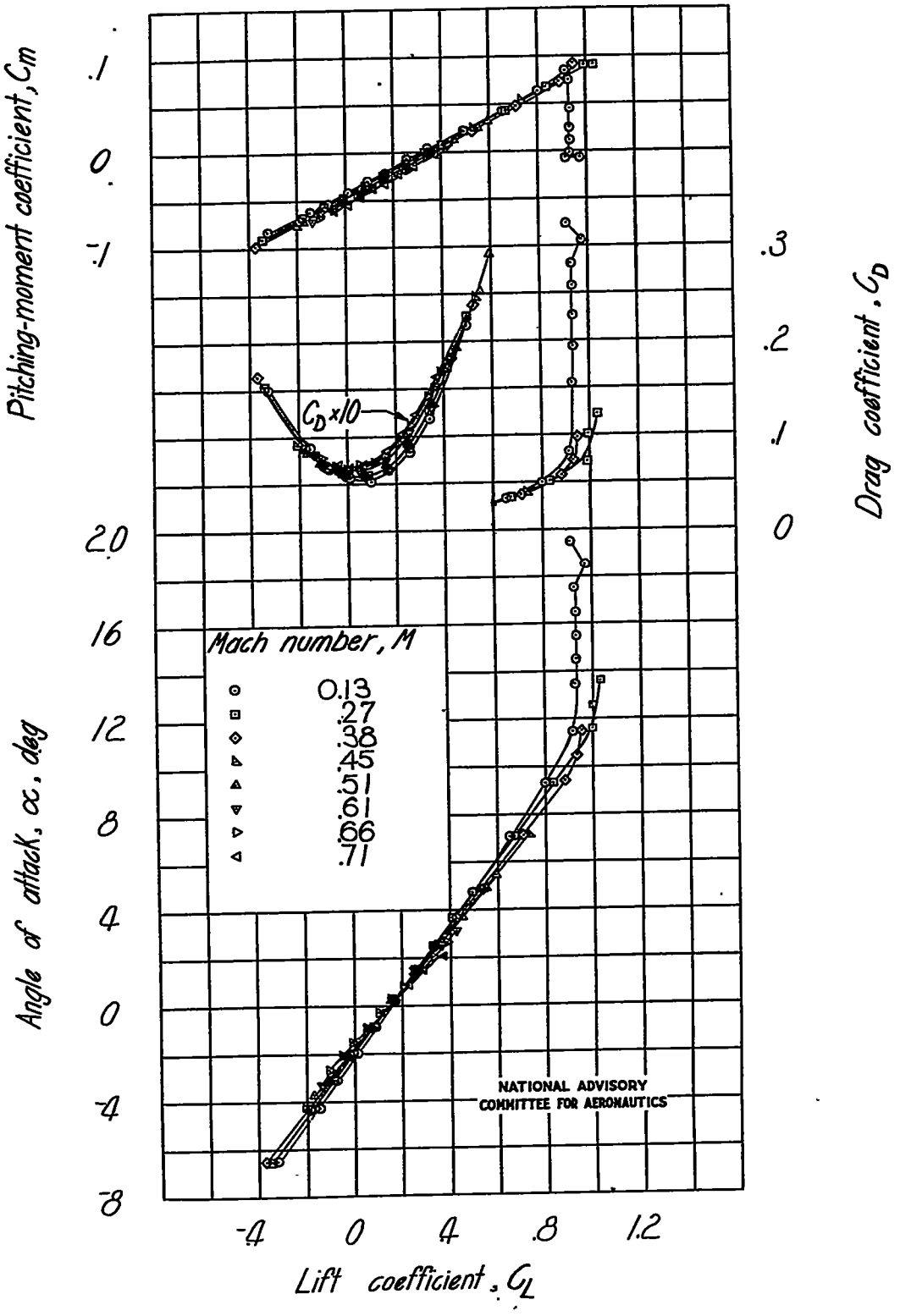

Figure 6.- Variation of plain-wing aerodynamic characteristics with Mach number.

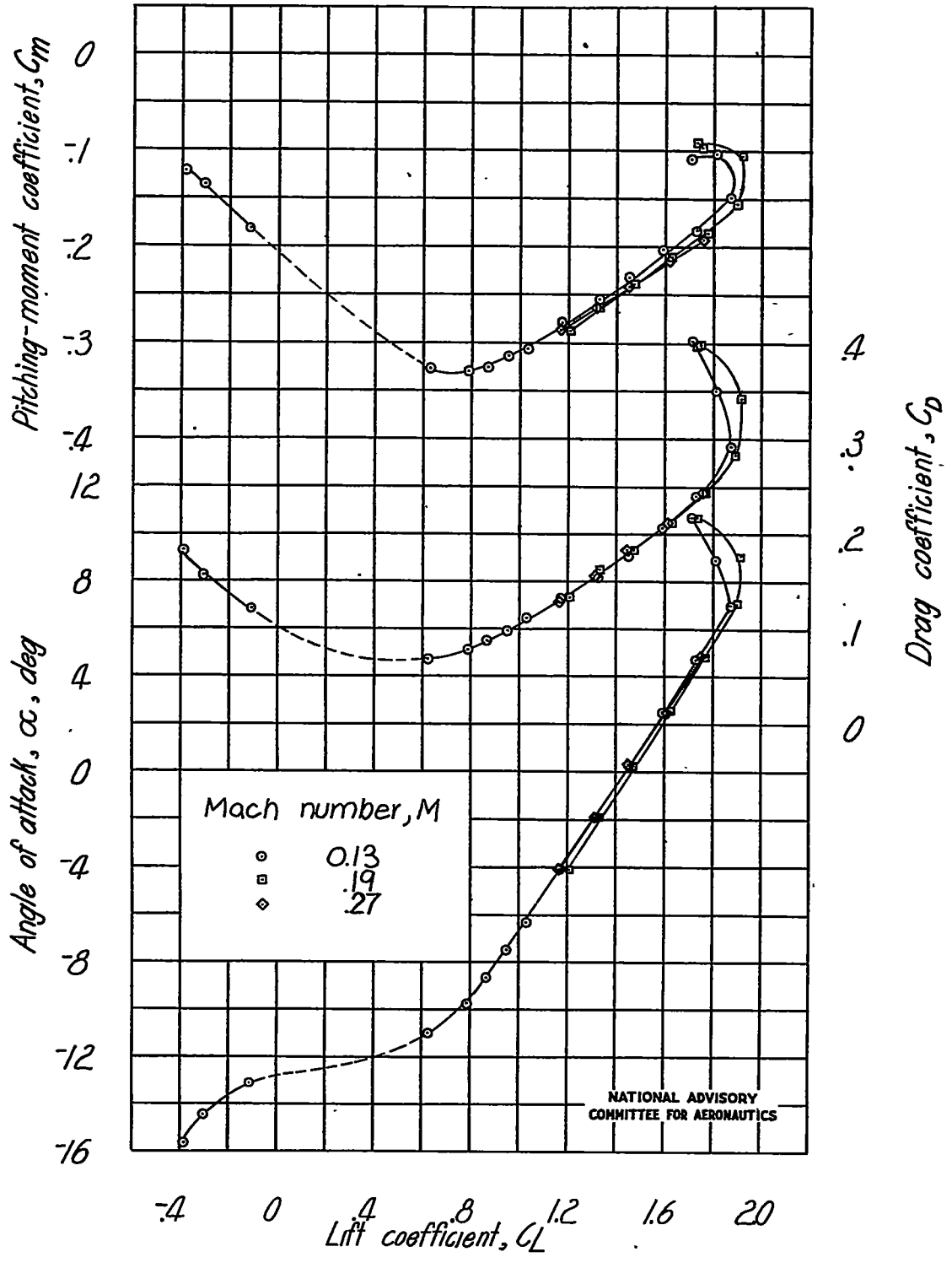

Figure 7.- Variation of aerodynamic characteristics with Mach number of wing with full-span slotted flap deflected 45°. Flap nose in normal location.

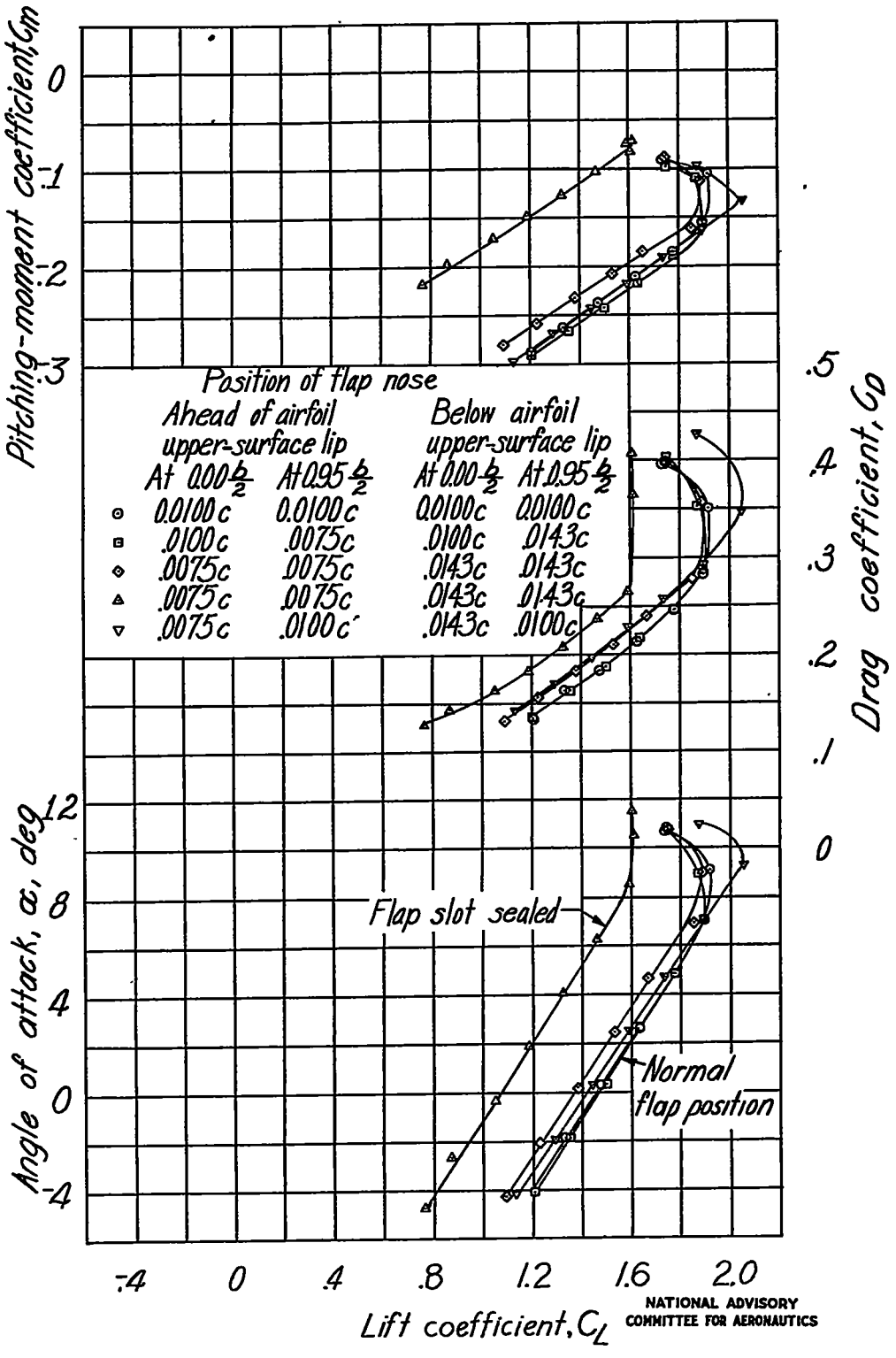

Figure 8.- Variation of aerodynamic characteristics of wing with full-span slotted flap deflected 45° and position of flap nose varied. M = 0.19.

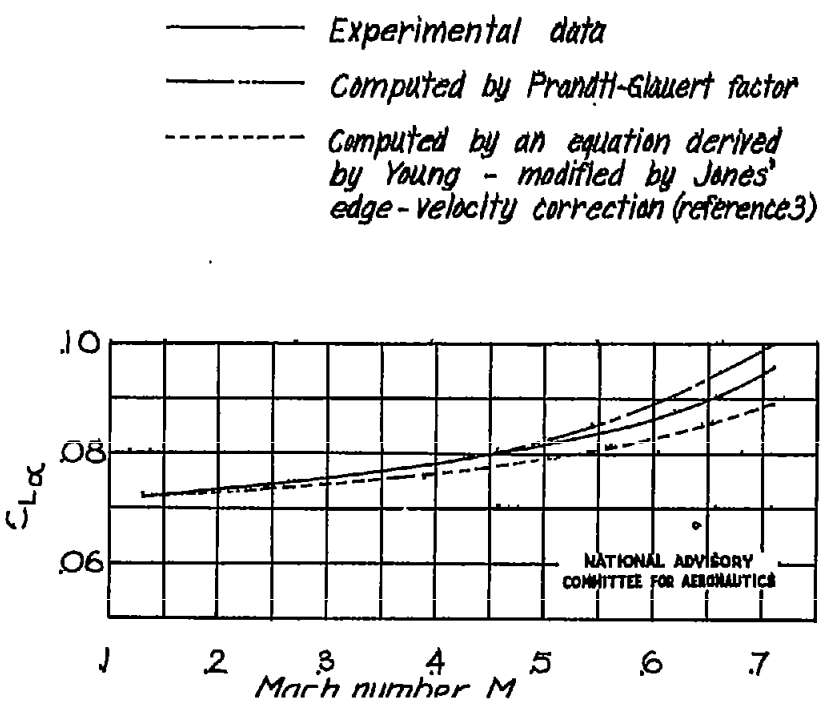

Figure 9.- Variation of measured and theoretical lift-curve slopes with Mach number.

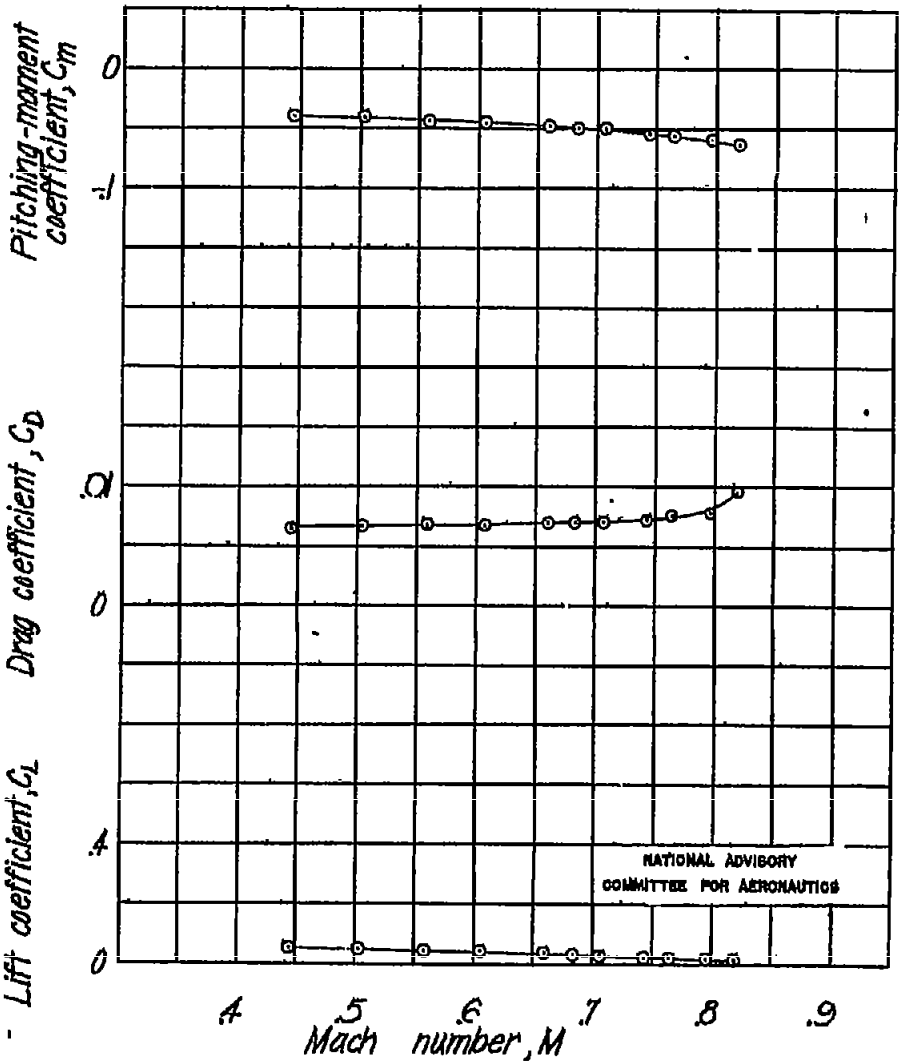

Figure 10.- Variation with Mach number of plain-wing characteristics. $\alpha = -1.45^\circ$.

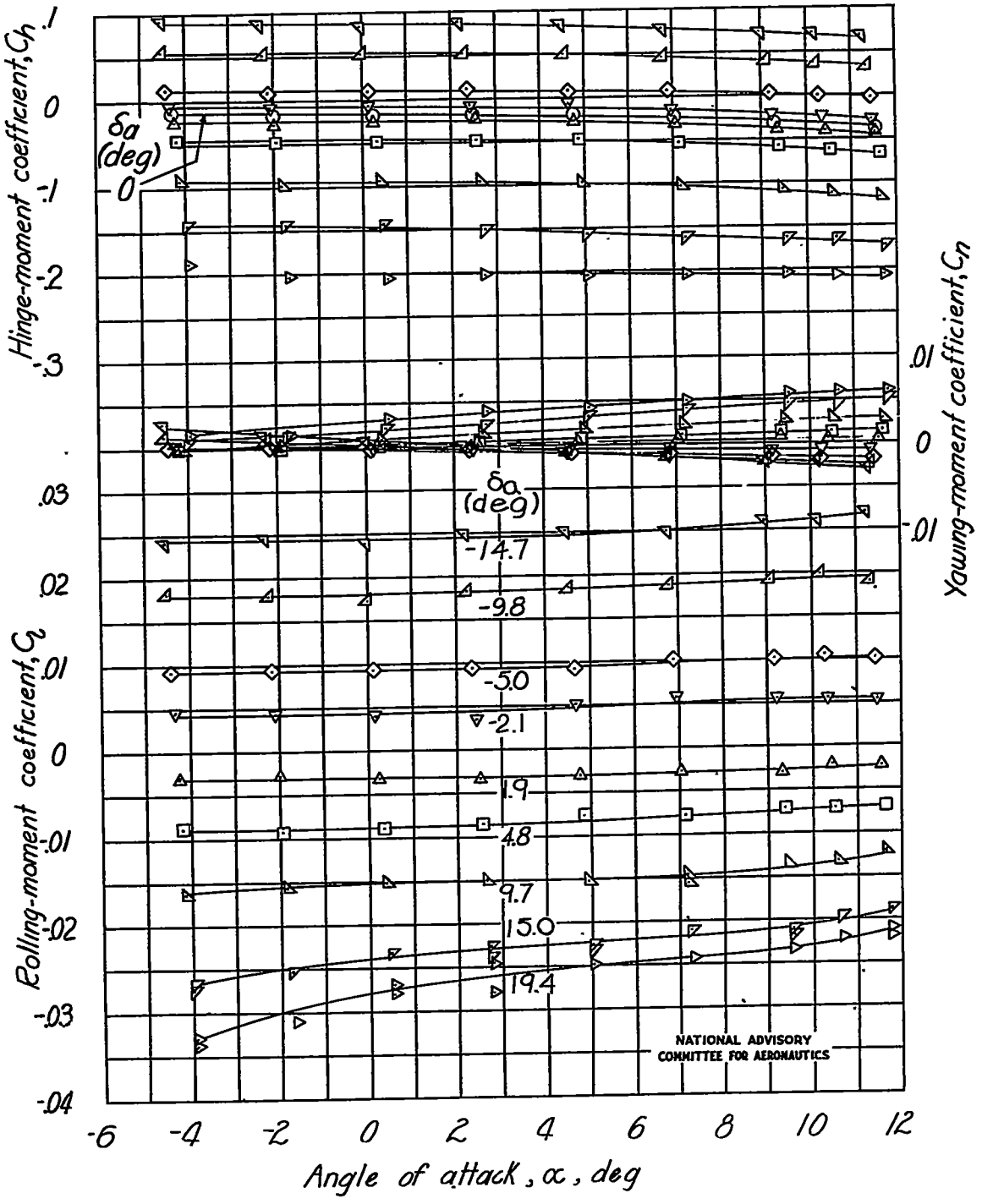

(a) Mach number, 0.27.

Figure 11.- Variation of lateral control characteristics of complete wing with aileron deflection. $\delta_f = 0$.

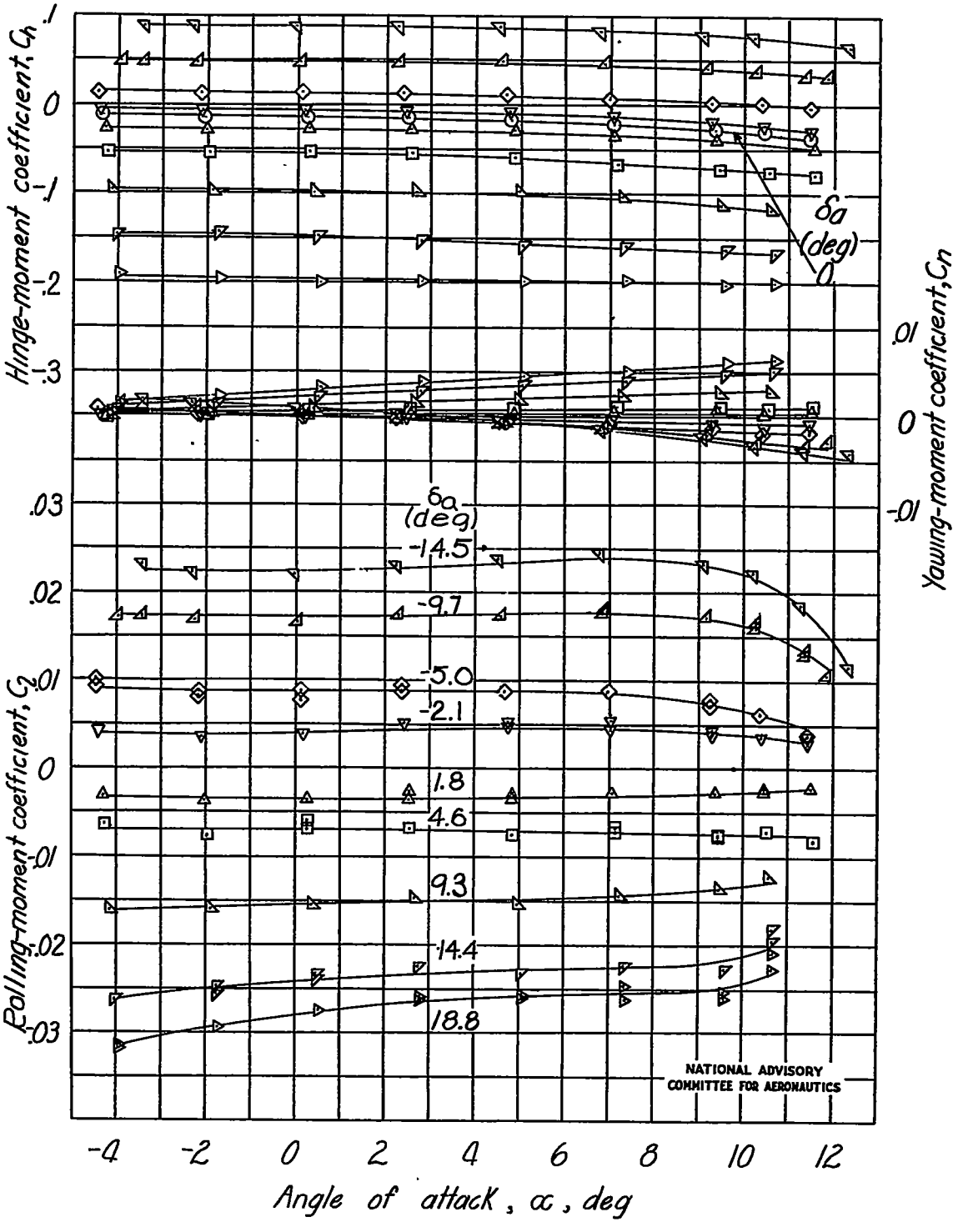

(b) Mach number, 0.38.

Figure 11.- Continued.

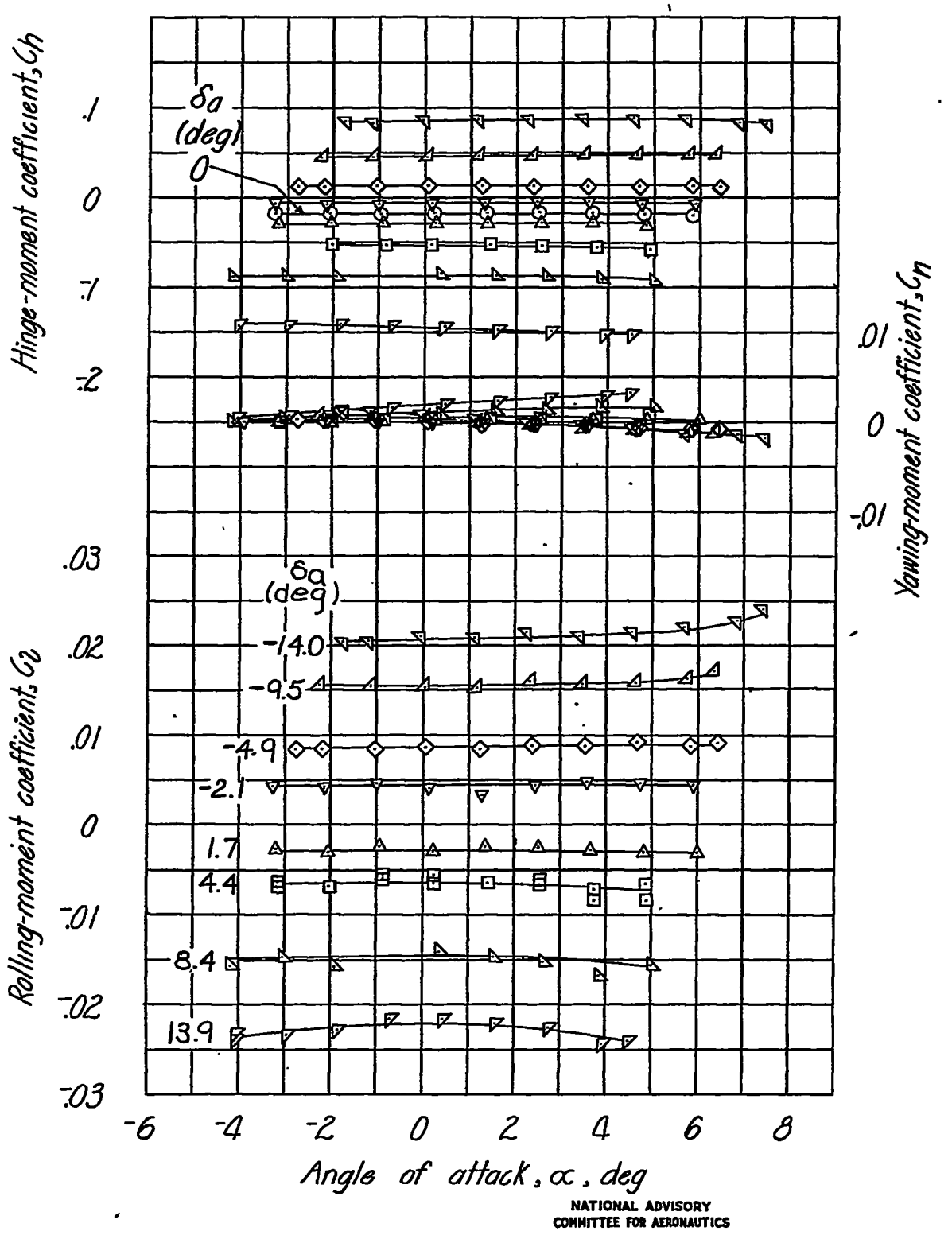

(c) Mach number, 0.51.

Figure 11.- Continued.

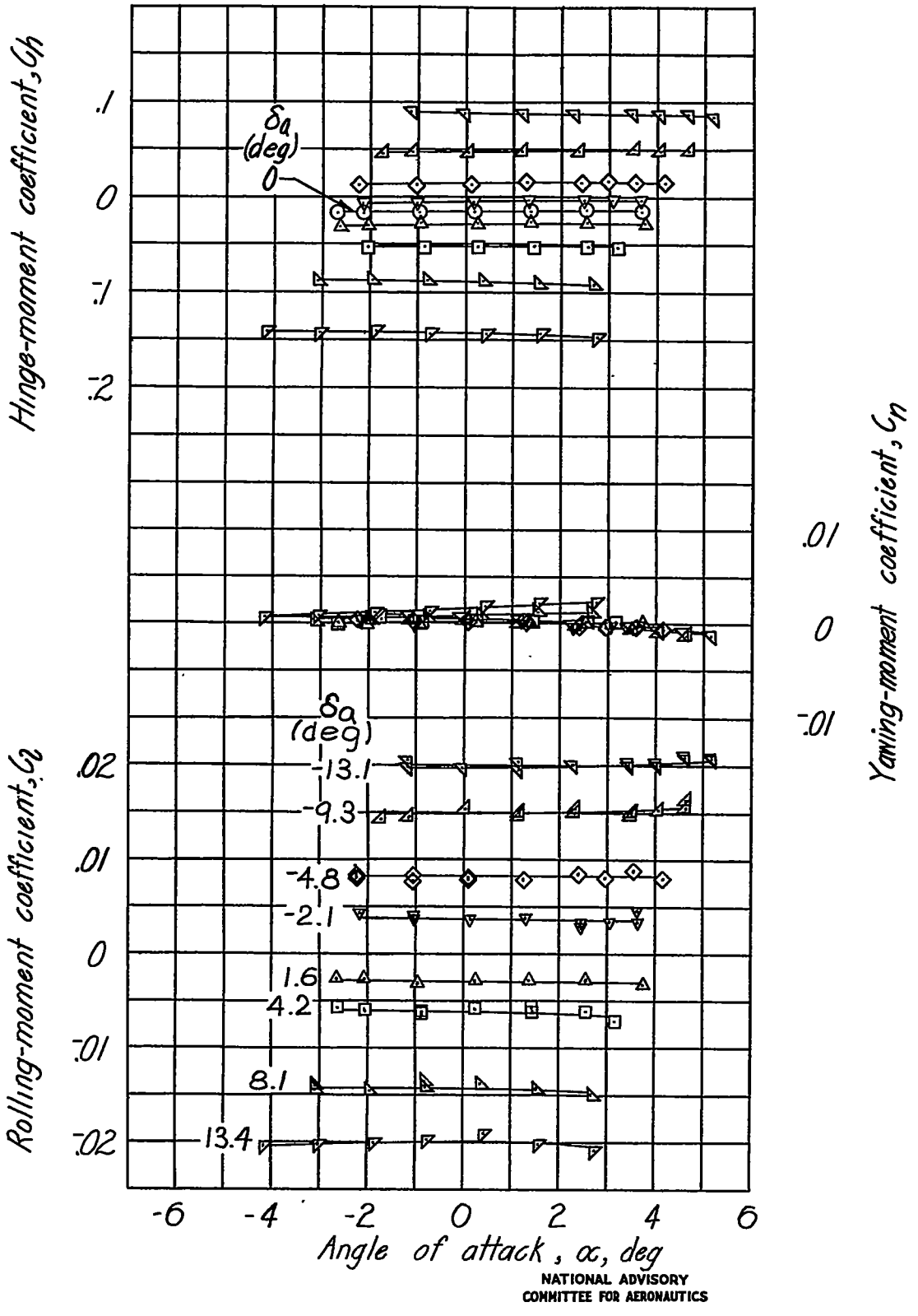

(d) Mach number, 0.61.

Figure 11.- Continued.

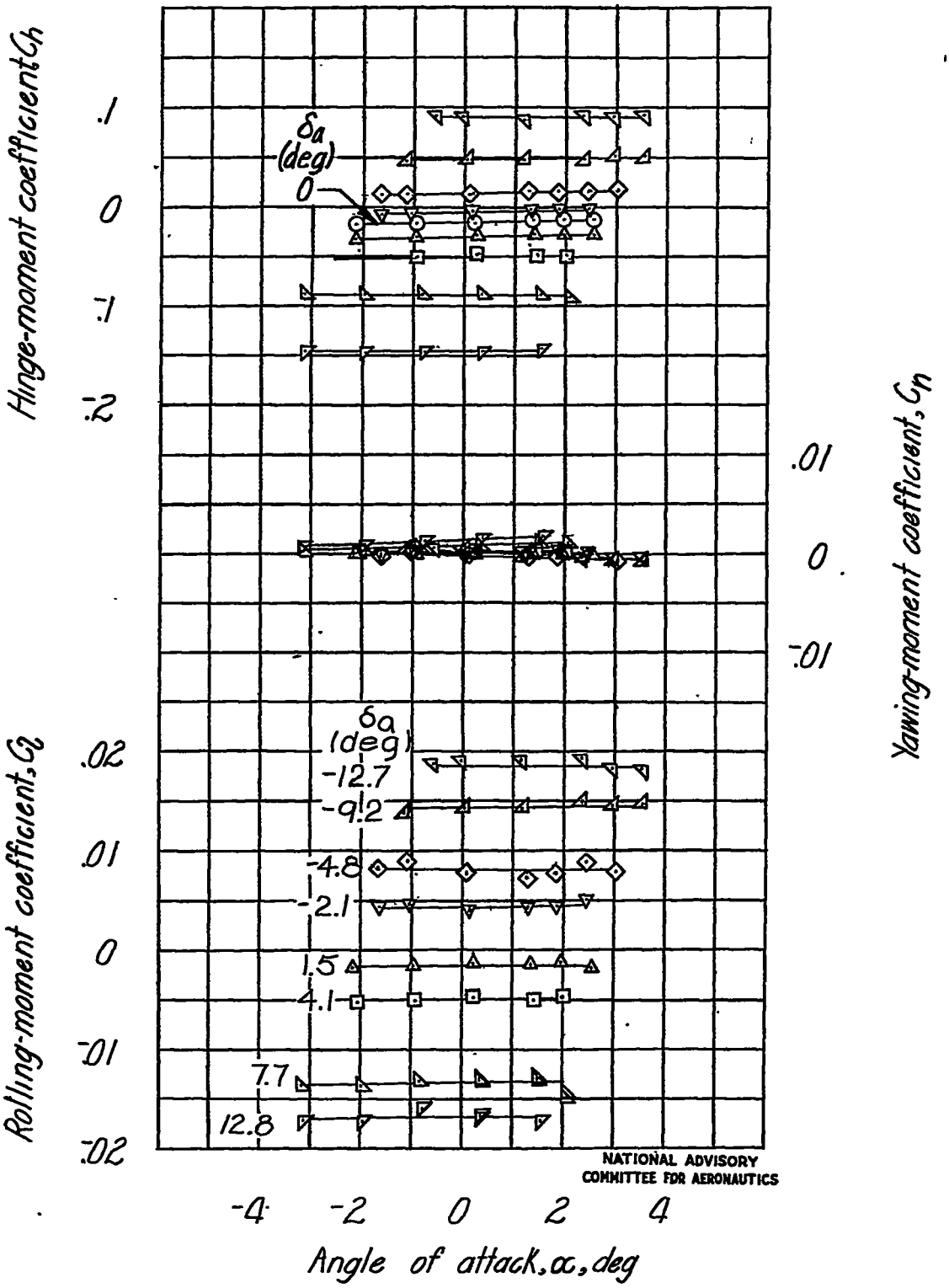

(e) Mach number, 0.71.

Figure 11.- Concluded.

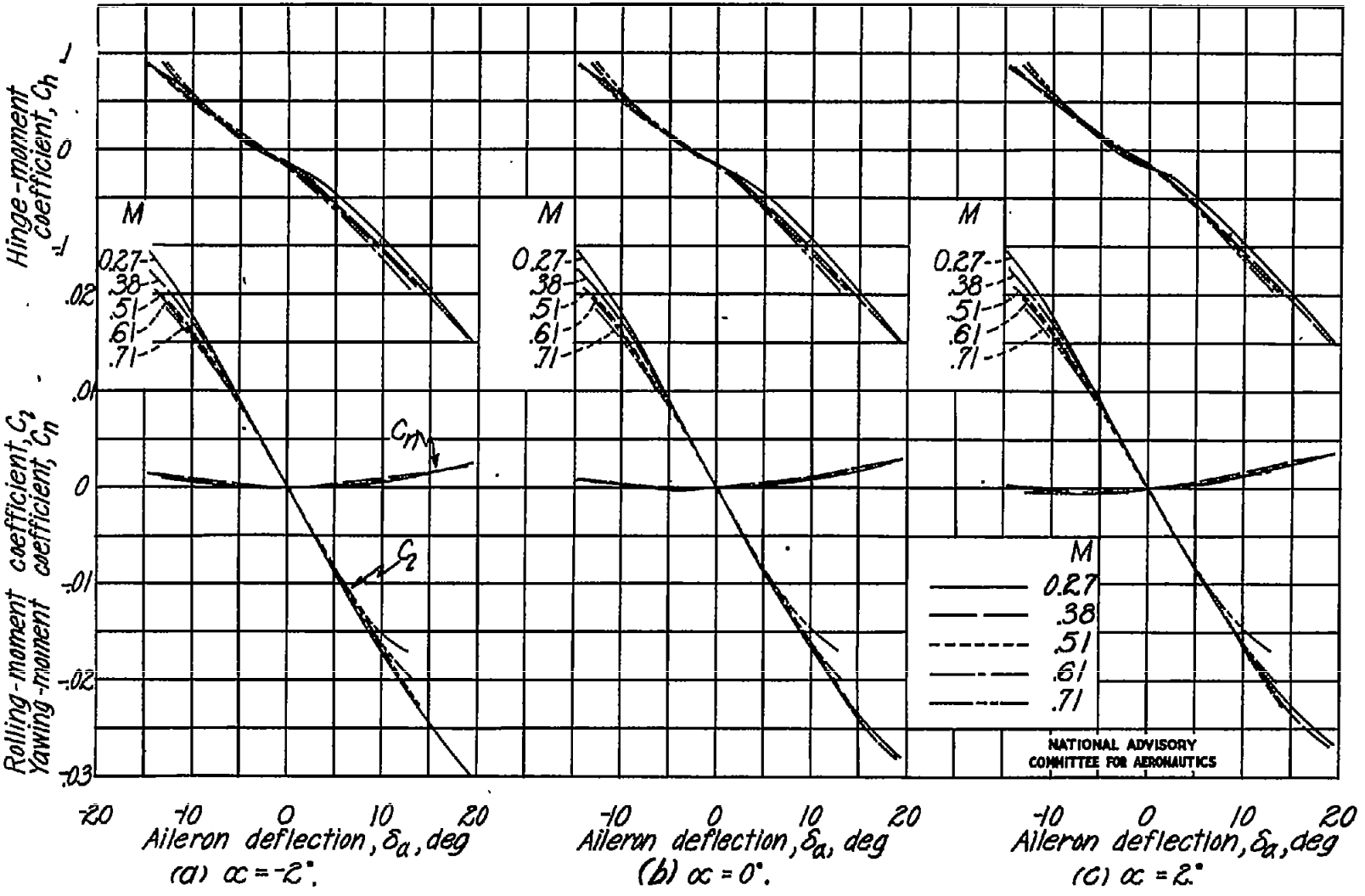

Figure 12.- Variation of lateral-control characteristics of complete wing with aileron deflection and Mach number. $\delta_f = 0°$.

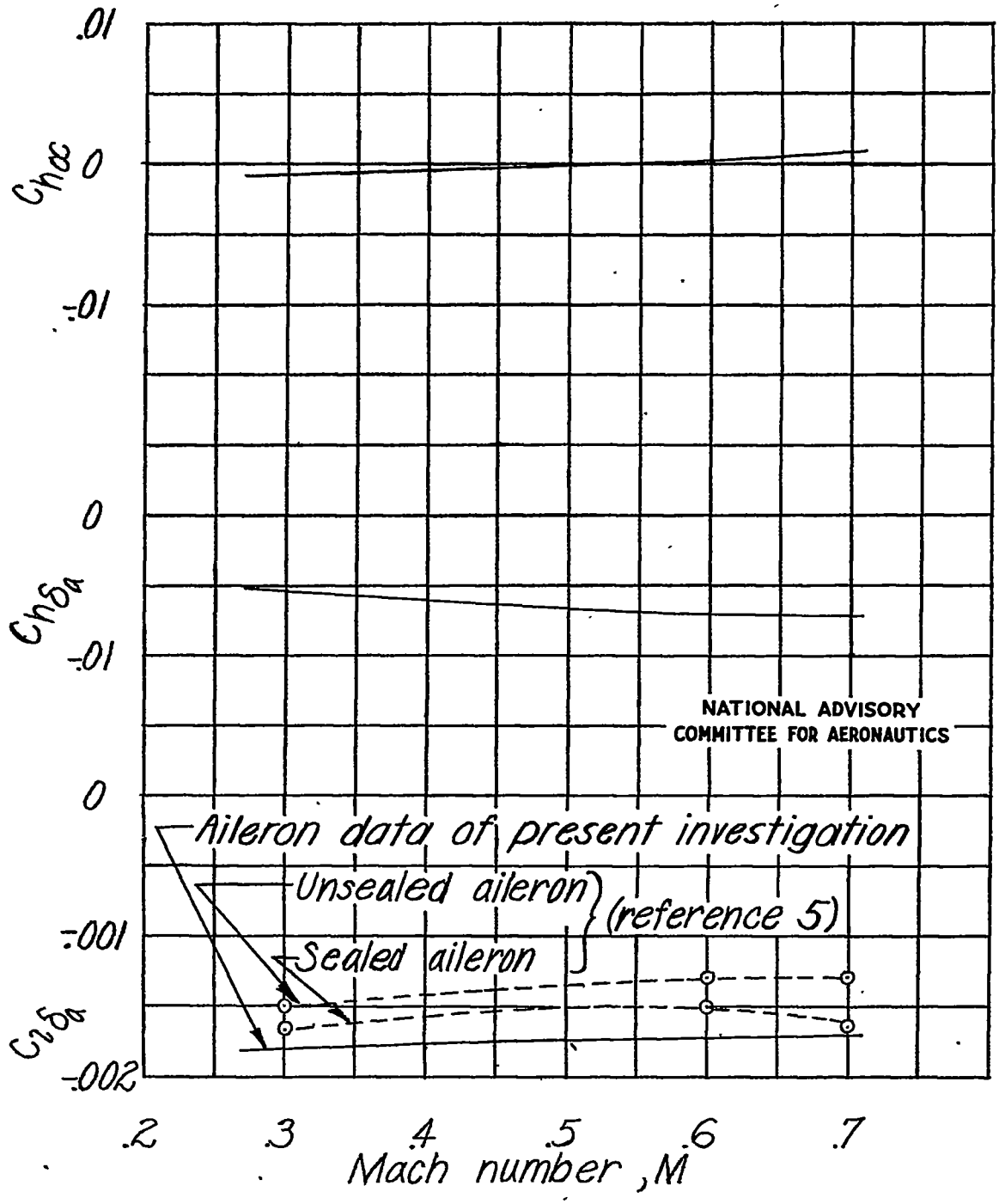

Figure 13.- Variation of parameters $C_{l_{\delta_a}}$, $C_{h_{\delta_a}}$, and C_{h_α} with Mach number.